Molecular Therapy
Nucleic Acids
Original Article

gRNA Sequence Heterology Tolerance Catalyzed by CRISPR/Cas in an *In Vitro* Homology-Directed Repair Reaction

Amanda M. Hewes,[1] Brett M. Sansbury,[1,2] Shaul Barth,[3] Gabi Tarcic,[3] and Eric B. Kmiec[1,2]

[1]Gene Editing Institute, Helen F. Graham Cancer Center & Research Institute, Christiana Care Health System, Newark, DE, USA; [2]Department of Medical and Molecular Sciences, University of Delaware, Newark, DE, USA; [3]Novellus, Jerusalem Bio-Park, 1st Kiryat Hadassah, Hadassah Ein-Kerem Medical Center Campus, Jerusalem, Israel, 9112001

CRISPR and associated Cas nucleases are genetic engineering tools revolutionizing innovative approaches to cancer and inherited diseases. CRISPR-directed gene editing relies heavily on proper DNA sequence alignment between the guide RNA (gRNA)/CRISPR complex and its genomic target. Accurate hybridization of complementary DNA initiates gene editing in human cells, but inherent gRNA sequence variation that could influence the gene editing reaction has been clearly established among diverse genetic populations. As this technology advances toward clinical implementation, it will be essential to assess what degree of gRNA variation generates unwanted and erroneous CRISPR activity. With the use of a system in which a cell-free extract catalyzes nonhomologous end joining (NHEJ) and homology-directed repair (HDR), it is possible to observe a more representative population of all forms of gene editing outcomes. In this manuscript, we demonstrate CRISPR/Cas complexation at heterologous binding sites that facilitate precise and error-prone HDR. The tolerance of mispairing between the gRNA and target site of the DNA to enable HDR is surprisingly high and greatly influenced by polarity of the donor DNA strand in the reaction. These results suggest that some collateral genomic activity could occur at unintended sites in CRISPR-directed gene editing in human cells.

INTRODUCTION

CRISPR and CRISPR-associated (Cas) nuclease systems localize to and cleave genomic DNA (gDNA) at a specific sequence with unprecedented efficiency that might enable clinical application.[1–4] Once the DNA target has been cleaved, DNA damage-response pathways and DNA repair processes are activated to ensure that the break sites are quickly and adequately repaired. In some cases, DNA resection and end ligation influence the generation of insertions and deletions (indels) that can lead to genetic disruption through the error-prone process of nonhomologous end joining (NHEJ). If an appropriate single-stranded DNA (ssDNA) or double-stranded DNA (dsDNA) repair template is present, then a different type of repair could take place. In aggregate, this form of repair has been termed homology-directed repair (HDR) because it relies on the genetic information provided by the donor DNA template to mend the break site.[5] In the normal lifespan of an organism, HDR occurs during and as a result of meiosis with sister chromatids crossing over or providing genetic information to repair a damaged site;[6] it is presumably error free. In human gene editing, it is anticipated that these HDR pathways will direct gene repair at a specific site and correct a genetic mutation.

Gene editing reactions rely on the stable binding of the gRNA to the chromosome site destined for cleavage and place the CRISPR/Cas complex in homologous alignment. For that reason, specific base pairing is essential in forming a stable complex proximal to a proto-spacer adjacent motif (PAM).[7] Previous data have suggested that gRNA activity is diminished when alterations are located approximately 4 to 13 bases adjacent to the PAM.[8–10] Sequence variation within the gRNA can enable both alternative cleavage activity and error-prone HDR at mismatched DNA binding sites if a suitable donor DNA template is present in the reaction. These studies suggest that CRISPR/Cas complexes can execute cleavage in the presence of imperfect or mismatched binding sites. A recent in-depth analysis suggested that genetic variance can alter CRISPR/Cas9 on-site targeting specificity.[11] Thus, genetic variation among and within populations[12] has the potential to modify CRISPR/Cas activity, particularly when there is imperfect (mismatched) sequence alignment between the gRNA and the target site. The importance of this problem can be illustrated by information gained from the 100,000 Genome Project, which has identified between 2,100 and 2,500 variants within an individual genome, including large deletions, insertions, point mutations, and inversions.[13,14] Sequence diversity within a population also has the potential to eliminate normal target sites and/or create unwanted target sites that can enable erroneous gene editing activity. This error-prone HDR involves the creation of aberrant insertions or deletions at the target site.

Received 27 February 2020; accepted 24 March 2020;
https://doi.org/10.1016/j.omtn.2020.03.012.

Correspondence: Eric B. Kmiec, PhD, Gene Editing Institute, Helen F. Graham Cancer Center & Research Institute, Christiana Care Health System, 4701 Ogletown-Stanton Road, Suite 4300, Newark, DE 19713, USA.
E-mail: eric.b.kmiec@christianacare.org

We have been analyzing gene editing in a cell-free *in vitro* system that affords us the opportunity to visualize the entirety of all genetic outcomes from a reaction. We expand these studies by analyzing how sequence heterology between the gRNA and the target site influences the frequency of precise HDR or error-prone HDR, which we define as indel formation. The focus has been primarily on understanding the mechanism of action and regulatory parameters surrounding the CRISPR Cas12a gene editing complex, particularly with regard to its tolerance for heterologous binding affinity. Our results demonstrate that HDR reactions not only proceed in the presence of mismatched DNA alignment, but also, under the right conditions, error-prone HDR can be promoted. Collateral genomic modification as a function of CRISPR-directed gene editing should raise caution about the widespread use of this technological approach in populations with diverse genetic backgrounds.

RESULTS

The effectiveness of CRISPR/Cas as a therapeutic agent is highly dependent on the alignment of the gene editing complex in perfect register with the target site. Altered or improper DNA hybridization is likely to limit success, as activity at misaligned pairing sites undoubtedly leads to mutagenesis. Whereas algorithms can assist in the design of the most efficient and precise gene editing tools, there is very limited information as to the functional consequences of CRISPR/Cas activity at imperfect binding sites even with optimal ribonucleoprotein (RNP) complexes. We know that the degree of mismatch between the target site and the gRNA sequence can affect the efficiency of DNA cleavage executed by the CRISPR/Cas complex.[8–10,15] Therefore, we took the next step by analyzing the functional consequences of this imperfect binding. We used an *in vitro* gene editing system, which incorporates an RNP designed to cleave the DNA at a designated site and a mammalian cell-free extract to catalyze both NHEJ and HDR in a single-reaction mixture. Single-stranded donor DNA fragments served as the repair template for precise HDR and imprecise genetic modifications (indels).[16,17] We had previously demonstrated that double-stranded DNA templates are less efficient in the *in vitro* system, particularly in reactions where HDR is the desired outcome; however, they serve as efficient donors when multiple CRISPR/Cas complexes are used.[16] This system allows us to visualize the wide array of products generated by CRISPR/Cas activity on target DNA.[18] As shown in Figure 1A, plasmid DNA is cleaved by an RNP composed of the appropriate gRNA and a Cas9 or Cas12a nuclease. After cleavage, the plasmid DNA is recovered, and the gene editing reaction is initiated by the addition of the cell-free extract and the donor DNA template. Plasmid DNA is recovered once more, transformed into bacteria, and isolated after genetic readout in bacteria. The DNA sequence analysis provides a profile of unaltered and altered DNA sequences at the target site. The readout system represents an array of products that were successfully transformed, since a single plasmid transforms a single bacterial cell and generates a unique colony.

We took a decidedly reductionist approach and recreated the mismatched binding between the gRNA of the RNP complex and the DNA target site in a validated model system. The beta galactosidase gene (*lacZ*) was targeted because it provides us the opportunity to measure the complete array of gene editing products through a simplified genetic readout system. We designed our RNP complex to induce DNA cleavage at position 1364, which if altered, leads to a blue to white color change. Figure 1B exhibits the coding region of the *lacZ* gene, the 1364 cut sites for both Cas9 and Cas12a nucleases, and the two single-stranded DNA oligonucleotides (ODNs) serving as donor fragments; Figure S1 shows the relationship of the *lacZ* gene within the pHSG299 plasmid. The donor DNA templates are shown above their region of complementarity and designated as 1364-NS to illustrate that the donor is identical to the nonsense strand and that 1364-S is identical to the sense strand of the target plasmid. Both donor templates span the same length of DNA and contain an 8-base *Not*I restriction site in the center, flanked by homology arms; one arm contains a 35-base stretch of DNA complementarity upstream (leftward), and the other contains 27 bases of complementary downstream (rightward). If successful and depending on which ODN is used, either the homolog or complement will be introduced into the top or bottom strand, and the repaired strand will then act as a template (after a second round of replication), generating a novel restriction site not previously present in pHSG299. Previous work has screened gene editing activity by *Not*I restriction enzyme digestion via gel electrophoresis.[17,18] The experimental plan was to utilize CRISPR/Cas9 and CRISPR/Cas12a, coupled individually to each of the DNA donor strands, to carry out gene editing on the *lacZ* gene.

The possible outcomes from each repair pathway for both CRISPR/Cas9 and CRISPR/Cas12a gene editing reactions are illustrated in Figure 1C. Cas9 generates blunt-end DNA cleavage products, whereas Cas12a produces staggered ends with 5 base, 5′ overhangs. Both types of cleavage products become susceptible to the DNA resection through NHEJ, microhomology-mediated end joining (MMEJ), and/or to modification by some form of HDR, such as single-stranded template repair (SSTR) and excision and corrective therapy (ExACT).[19,20] We recognize that there may be several recombination/repair pathways under the general heading of HDR; therefore, we scored the exact and inheritable placement of the complement of the *Not*I sequence into the target site as HDR. It is likely that HDR and NHEJ reactions occur within a single reaction mixture and that DNA changes can be catalyzed by some form of error-prone HDR or NHEJ. These types of product molecules would fall under the category of indels.

The results of *in vitro* gene editing reactions promoted by Cas9 or Cas12a, 1364-NS and 1364-S donor DNA, and wild-type gRNA (no mutations/base changes) are displayed in Figure 2. Below each sequencing alignment are several trace files of data obtained in these experiments illustrating that indel formation is generated by CRISPR/Cas gene editing and not by failed DNA sequencing reactions. Overall, Cas12a enables a high percentage of precise HDR

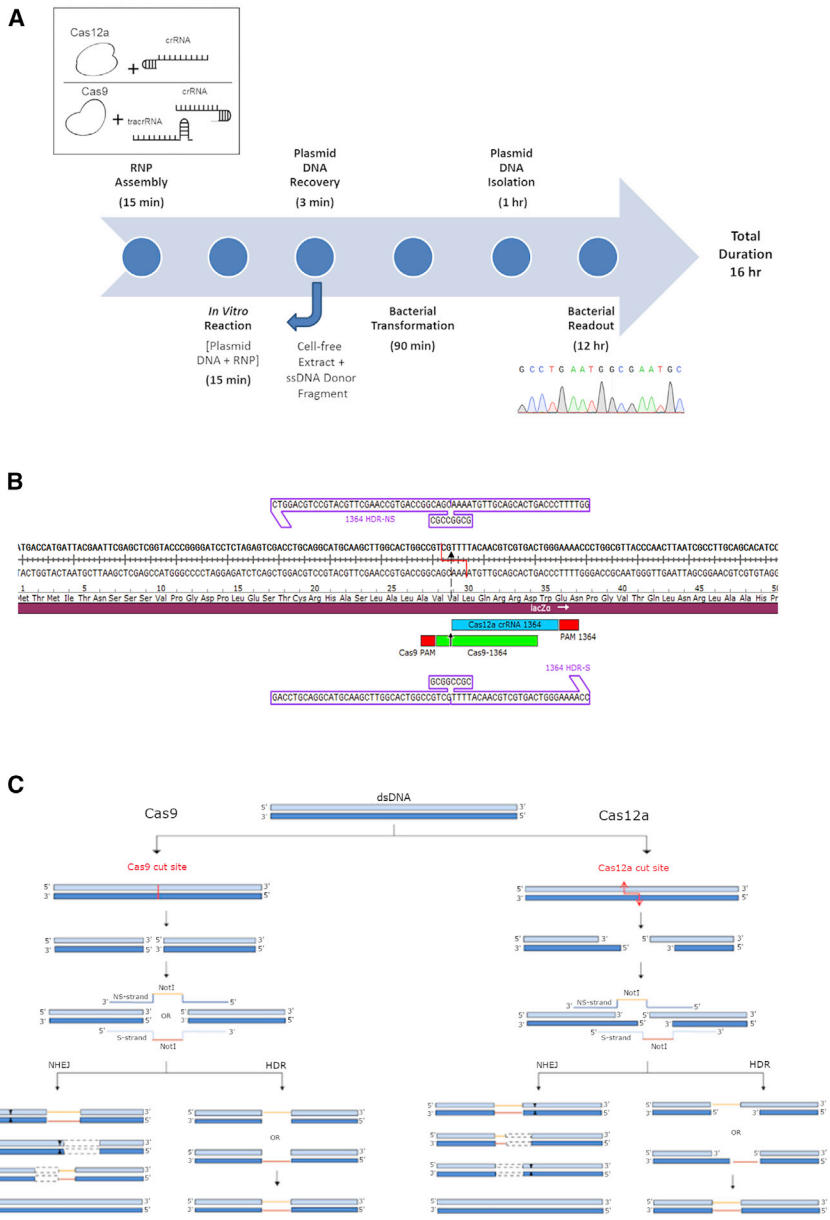

Figure 1. Gene Editing Assay System

(A) Cas12a or Cas9 nuclease is combined with its appropriate gRNA to form the ribonucleoprotein (RNP) complex. After Cas12a/Cas9 RNP has been constructed, plasmid DNA is added to the reaction. DNA is recovered by silica spin columns, and then single-stranded ODN and cell-free extract are added to the reaction. The DNA is recovered once more by silica spin columns and undergoes bacterial transformation. The colony readout is observed the following day, and the colonies can further be analyzed by Sanger sequencing. The total duration of the *in vitro* reaction takes approximately 16 h to complete. (B) Cas12a and Cas9 gRNAs are illustrated below the wild-type *lacZ* sequence showing overlap between the two gRNAs at the 1364 cut site. Cas12a creates a staggered double-stranded (ds)DNA break shown by a staggered red line, whereas Cas9 creates a blunt-ended dsDNA break illustrated by a dotted black arrow. The 1364 sense strand and 1364 nonsense strands are located in the diagram to their complementary sequences of the *lacZ* gene. (C) A wild-type dsDNA fragment is represented at the top, which divides Cas9 and Cas12a reactions. (Left) Cas9, creating a single, blunt-ended dsDNA cut shown with a bold red line. A complementary ssDNA donor fragment of the sense or nonsense polarity will serve as a template containing an 8-base *Not*I restriction enzyme site to repair the break site. (Right) Cas12a creates a staggered dsDNA cut, causing a 5-base pair, 5′ overhang, illustrated by the staggered red arrow. After the dsDNA break occurs, the sense strand or the nonsense single-stranded donor fragment will serve as a template to incorporate the 8-base pair *Not*I restriction enzyme site. When nonhomologous end joining occurs, insertions represented by black triangles, deletions represented by dotted boxes, or wild-type DNA sequences result. When homology-directed repair occurs, the *Not*I site is incorporated on one side of the DNA precisely, and then this strand becomes the template to repair the other strand by replication machinery.

activity, whereas only indels were found when Cas9 generated site-specific cleavage with the 1364-NS donor DNA template (Figure 2A). All Cas9-catalyzed product molecules exhibit various levels of deletions, two and five bases primarily. For each independent reaction, approximately 20 to 26 blue colonies were also sequenced to serve as internal controls; all blue colonies harbored a plasmid molecule with the unedited wild-type sequence. When the 1364-S strand was used as the donor DNA template, Cas12a-catalyzed reactions once again produced a combination of molecules comprising precise HDR and molecules bearing indels (Figure 2B). CRISPR/Cas9 1364-S-catalyzed reactions produced two types of outcomes: first, a low level of HDR, and second, a high level of indel formation, mimicking the results attained in the experiments carried out in the Cas9/1364-NS reactions above. Table 1 provides a summary of the gene editing activity of CRISPR/Cas9 and CRISPR/Cas12a with the two donor DNA templates. Taken together, these two sets of reactions serve as the base level of HDR activity when the gRNA and the target site are completely complementary. It should be noted that we routinely find a low number of white colonies with the combination of CRISPR/Cas12a with the S-strand ODN. The results indicate the versatility of the *in vitro* system that enables visualization of a wide range of gene editing products.

Sequence Heterology and CRISPR-Directed DNA Cleavage

To address the tolerance of mismatched bases or heterology in HDR reactions, we created a series of gRNAs bearing 1, 2, 3, 4, or 5 mismatches out of 20 or 21 bases, for Cas9 or Cas12a, respectively, in the center (center mutations). In the top panels of Figure 3A (top

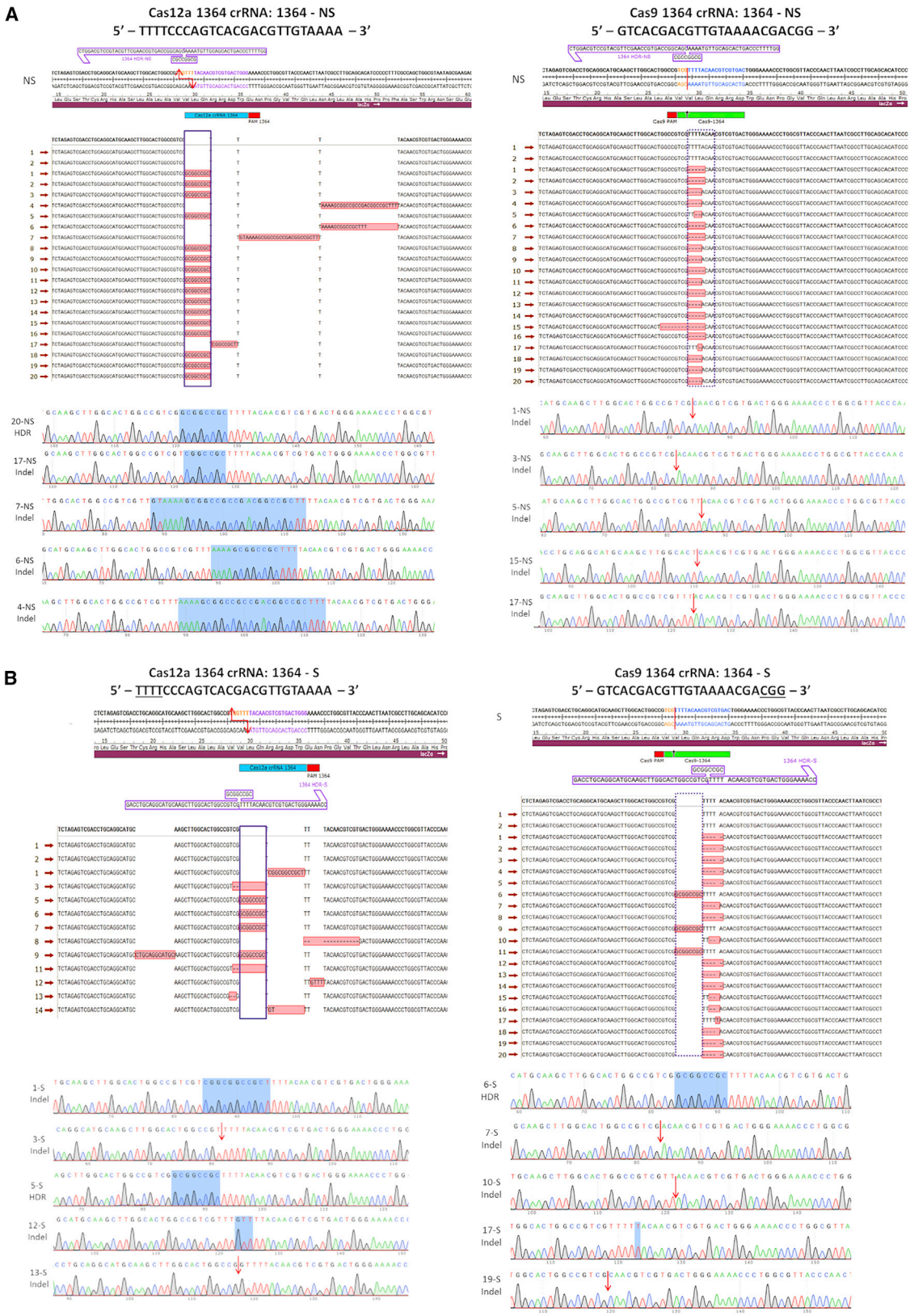

(legend on next page)

Table 1. CRISPR/Cas12a and Cas9 Base-Level Homology-Directed Repair Activity Using Both Donor DNA Templates

Cas12a 1364 HDR-NS: 1364 WT crRNA					Cas9 1364 HDR-NS: 1364 WT crRNA				
Colony	Total	HDR	Indel	WT	Colony	Total	HDR	Indel	WT
White	20	16	4	0	white	20	0	20	0
Blue	26	0	0	26	blue	25	0	0	25
Cas12a 1364 HDR-S: 1364 WT crRNA					Cas9 1364 HDR-S: 1364 WT crRNA				
Colony	Total	HDR	Indel	WT	Colony	Total	HDR	Indel	WT
White	11	3	8	0	White	20	2	18	0
Blue	20	0	0	20	Blue	22	0	0	22

The total number of blue and white colonies sequenced for base-level *in vitro* reactions using CRISPR/Cas12a and CRISPR/Cas9 and the 1364-NS and 1364-S donor template strands are shown. The sequences harboring products of homology-directed repair, insertion/deletions (error-prone sequences), and/or wild-type (WT) molecules are shown.

panels), we describe the type of nucleotide base change, either purine to pyrimidine or vice versa, to generate the mismatch to the target site. The bottom panels of Figure 3A display the center mutation profile of both the CRISPR/Cas12a and CRISPR/Cas9 gRNA sequence in relation to the PAM site, which will help form the RNP complexes.

We tested the impact of center mutations in the gRNA on the DNA cleavage reaction, promoted by either Cas12a or Cas9, and show the products of the cleavage reactions in Figure 3B (right panel). With CRISPR/Cas12a, complete linearization is observed in the perfectly matched gRNA sequence, as well as the sequence bearing one mismatch to the target site. In the reaction mixture containing 2 base mismatches, most of the resulting DNA appears to be linearized, but a small amount, illustrated by a thin band, is observed at the nicked position. The nicked DNA band becomes more prominent as the sequence heterology increases by 3 or 4 bases, respectively, in Cas12a-promoted reactions. A 5-base mismatch does not facilitate nicked or linearized DNA and remains intact plasmid DNA. Reactions catalyzed by CRISPR/Cas9 generate linear DNA, starting with a wild-type gRNA (no mutations), and continue throughout the reaction, including gRNA/target DNA combinations with 4 mismatched base pairs; a slight increase in nicked DNA is also seen as the number of mismatched bases increases. Like Cas12a, 5 mismatches between the gRNA and the target plasmid resulted in very little detectable cleavage activity. Taken together, our data suggest that CRISPR/Cas9 RNPs are more tolerant to gRNA heterology in the generation of linearized DNA than the Cas12a RNP.

gRNA Variance and the HDR Reaction

We carried out the same reaction described in Figure 2, except in this case, there were 1, 2, 3, 4, or 5 base mismatches between the gRNA and the target site in the plasmid DNA. Table 2 (left) displays the outcome of functional HDR activity promoted by CRISPR/Cas12a with the 1364-S ODN. For each reaction, we sequenced between 20 and 21 blue colonies and between 11 and 20 white colonies. It should be noted that with 4 or 5 mismatches, there were very few, if any, white colonies observed; thus, analyses of HDR or indel activity were difficult to assess. The presence of one or two mismatches reduces the number of precise HDR events dramatically compared to no mismatches and across all center mutations; the dominant products were found to be indels (sequencing alignment data in Figure S2A). Overall, low levels of HDR events are observed with 5 of the 6 reaction mixtures where the donor template 1364-S was used. Table 2 (right) displays the results of an identical reaction mixture, where Cas9 served as the programmable nuclease in each case; Figure S2B shows the sequencing alignments for each reaction. The level of precise HDR activity surprisingly increases as a function of heterology when Cas9 serves as the nuclease; overall indel formation decreases as the number of mismatches increases from 0 to 3. Even with 4 mismatched bases, three of the ten modified DNA molecules contain precise HDR events. Figures 4A and 4B show the genotypic profiles and the position of the indels for the population of product molecules generated by the 2- and 4-base mismatches between the gRNA and the target site. DNA heterology appears to impact the reactions catalyzed by Cas12a and the S strand at a greater degree than the comparable reaction of Cas9 and the S strand. On rare occasions, a wild-type sequence can be generated; even though the colony appears to be white, it is most likely due to a loss of the indicator dye.

Previous data have pointed to the importance of strand bias in the gene editing reaction,[17] and many studies have demonstrated that the polarity of the ssDNA can affect the frequency of gene repair.[21–25] Based on these data, we carried out similar experiments where we substituted the donor DNA template for the opposite polarity. The experiments

Figure 2. CRISPR/Cas12a and Cas9 Homology-Directed Repair

The Cas12a (left) and Cas9 (right) 1364 wild-type gRNA sequences are shown. The homology-directed repair (A) nonsense and (B) sense single-stranded oligonucleotides with homology arms are shown to their complementary region in the *lacZ* gene. The target sequence in the *lacZ* gene is shown in purple, and the 5-base pair, 5′ overhang created by the Cas12a ribonucleoprotein (RNP) is shown in orange with a staggered red arrow. The target sequence is shown in blue, and the blunt-ended double-stranded DNA break is indicated by a solid red line for Cas9. The solid and dotted purple boxes outline the regions where the 8-base pair *Not*I site will be incorporated if homology-directed repair occurs. Five trace files are shown below each sequencing alignment; highlighted blue sections show either precise homology-directed repair or insertions/deletions, and red arrows indicate where deletions occurred.

A

Cas12a Center Mutations: Base Changes	
C1	Purine, → Pyrimidine
C2	Purine, Pyrimidine → Pyrimidine, Purine
C3	Purine, Pyrimidine, Purine → Pyrimidine, Purine, Pyrimidine
C4	Purine, Pyrimidine, Purine, Purine → Pyrimidine, Purine, Pyrimidine, Pyrimidine
C5	Purine, Pyrimidine, Purine, Purine, Pyrimidine → Pyrimidine, Purine, Pyrimidine, Pyrimidine, Purine

Cas9 Center Mutations: Base Changes	
C1	Pyrimidine → Purine
C2	Pyrimidine, Purine → Purine, Pyrimidine
C3	Pyrimidine, Purine, Pyrimidine → Purine, Pyrimidine, Purine
C4	Pyrimidine, Purine, Pyrimidine, Pyrimidine, → Purine, Pyrimidine, Purine, Purine
C5	Pyrimidine, Purine, Pyrimidine, Pyrimidine, Purine → Purine, Pyrimidine, Purine, Purine, Pyrimidine

Cas12a crRNA 1364 Center Mutations				
	5′→3′ PAM	5′→3′ crRNA	Base Change	New Variations
WT	TTTT	CCCAGTCACGACGTTGTAAAA	No Change	CCCAGTCACGACGTTGTAAAA
C1	TTTT	CCCAGTCACGACGTTGTAAAA	A→C	CCCAGTCCCGACGTTGTAAAA
C2	TTTT	CCCAGTCACGACGTTGTAAAA	AC→CA	CCCAGTCCAGACGTTGTAAAA
C3	TTTT	CCCAGTCACGACGTTGTAAAA	ACG→CAT	CCCAGTCCATACGTTGTAAAA
C4	TTTT	CCCAGTCACGACGTTGTAAAA	ACGA→CATC	CCCAGTCCATCCGTTGTAAAA
C5	TTTT	CCCAGTCACGACGTTGTAAAA	ACGAC→CATCA	CCCAGTCCATCAGTTGTAAAA

Cas9 crRNA 1364 Center Mutations				
	5′ → 3′ PAM	5′→3′ crRNA	Base Change	New Variations
WT	CGG	GTCACGACGTTGTAAAACGA	No Change	GTCACGACGTTGTAAAACGA
C1	CGG	GTCACGACGTTGTAAAACGA	C→G	GTCACGAGGTTGTAAAACGA
C2	CGG	GTCACGACGTTGTAAAACGA	CG→GC	GTCACGAGCTTGTAAAACGA
C3	CGG	GTCACGACGTTGTAAAACGA	CGT→GCA	GTCACGAGCATGTAAAACGA
C4	CGG	GTCACGACGTTGTAAAACGA	CGTT→GCAA	GTCACGAGCAAGTAAAACGA
C5	CGG	GTCACGACGTTGTAAAACGA	CGTTG→GCAAC	GTCACGAGCAACTAAAACGA

B

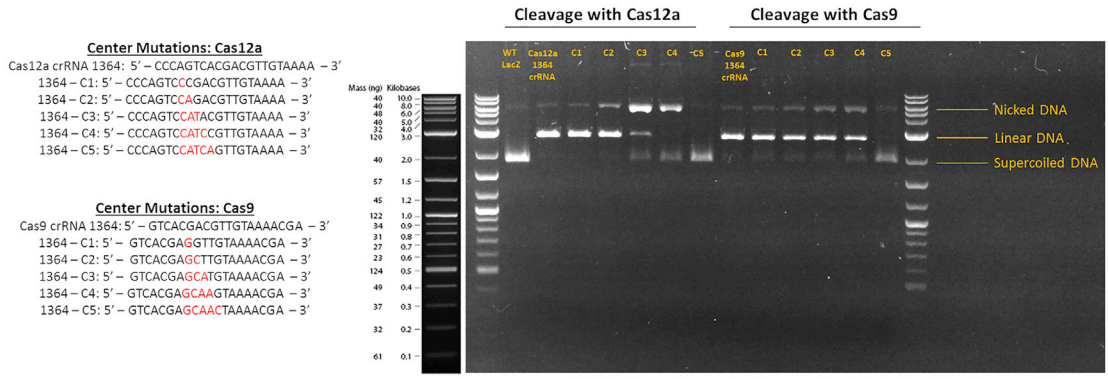

Figure 3. CRISPR/Cas12a and Cas9 Center Mutation Design and Cleavage Activity

(A) (Top) Base changes from purine to pyrimidine (and vice versa) for Cas12a and Cas9 center mutations are shown. (Bottom) The designs of the Cas12a/Cas9 1364 gRNA center mutations, along with the wild-type 1364 gRNA sequence. (B) The 1364 gRNA sequences with the intended center mutations one through five (C1–C5) for both Cas12a and Cas9 nucleases in the 5′-to-3′ direction are shown. An agarose gel is shown, demonstrating the cleavage activity of the center mutation gRNA ribonucleoproteins with a 1-kb ladder.

shown in Table 3 contained reaction mixtures with CRISPR/Cas12a and CRISPR/Cas9 coupled individually with the 1364-NS donor template (sequencing alignment data in Figures S2C and S2D). HDR appears to occur sporadically when there are two or four mismatches between the gRNA and the target DNA. The genetic profile in each of the gene editing reactions is quite different when Cas12a provides the nuclease function and coupled with the NS strand. High levels of precise HDR occur even when one, two, or three mismatches between the gRNA and the target site exist. Figure 5A demonstrates the high level of HDR when three mismatches are present using a CRISPR/Cas12a RNP in conjunction with the NS donor DNA template. In contrast, HDR takes place at lower levels when the combination CRISPR/Cas9 and the NS donor DNA template catalyze the reaction; Figure 5B displays these lower levels of HDR when two mismatches are present. These data suggest that Cas12a, with the 1364-NS single-stranded donor DNA template, produces a high percentage of precise HDR activity, even in the presence of multiple mismatches between the gRNA and the target site. Taken together, our data indicate that the CRISPR/Cas12a complex is more efficient in the catalysis of HDR when compared to the CRISPR/Cas9 complex under identical conditions using the NS donor DNA template. Therefore, we carried out Fisher's exact test to compare both CRISPR/Cas complexes when they align in perfect register with the target site and contain the NS donor DNA template and when the gRNAs contain 1, 2, or 3 mismatches. As seen in Table 4, there is a statistically significant difference between the two CRISPR/Cas complexes under each of these reaction conditions, as reflected by the *P*-values. However, when a similar comparison was carried out, evaluating only CRISPR/Cas12a complexes bearing 0, 1, 2, or 3 mismatched base pairs, no statistically significant differences were found; each of these conditions contained a *P*-value greater than 0.01. This demonstrates that efficient HDR takes place whether the gRNA and target site are perfectly aligned or contain up to 3 mismatched base pairs reflecting a surprisingly high level of tolerance for sequence heterology in Cas12a-driven reactions.

Table 2. CRISPR/Cas12a and Cas9 Homology-Directed Repair Sense Strand Center Mutations

Cas12a 1364 HDR-S: Center Mutations						Cas9 1364 HDR-S: Center Mutations					
Mutation	Colony	Total	HDR	Indel	WT	Mutation	Colony	Total	HDR	Indel	WT
C0	White	11	3	8	0	C0	White	20	2	18	0
C0	Blue	20	0	0	20	C0	Blue	22	0	0	22
C1	White	9	1	8	0	C1	White	20	0	20	0
C1	Blue	20	0	0	20	C1	Blue	22	0	0	22
C2	White	8	1	6	1	C2[a]	White	20	2	18	0
C2	Blue	21	0	0	21	C2	Blue	21	0	0	21
C3	White	6	0	6	0	C3	White	10	2	8	0
C3	Blue	21	0	0	21	C3	Blue	22	0	0	22
C4	White	0	0	0	0	C4[a]	White	10	3	7	0
C4	Blue	21	0	0	21	C4	Blue	22	0	0	22
C5	White	0	0	0	0	C5	White	0	0	0	0
C5	Blue	20	0	0	20	C5	Blue	22	0	0	22

The total number of blue and white colonies is represented, along with the number of colonies found to have precise homology-directed repair, insertions or deletions (error-prone sequences), or wild-type molecules for Cas12a (left) and Cas9 (right) center mutations using the single-stranded oligonucleotide of the sense polarity.
[a]Unique and precise homology-directed repair event.

DISCUSSION

CRISPR-directed gene editing is highly dependent on the alignment of the CRISPR complex and the target DNA sequence in homologous register. Previous reports have indicated that some degree of mismatched base pairing between the gRNA and the DNA destined for cleavage can be tolerated; in fact, it does not prohibit efficient double-strand DNA breakage.[8–10,15,26,27] These important studies provide insight on the potential for nonspecific CRISPR/Cas activity and off-site mutagenesis. Here, we examine the tolerance of mismatched DNA bases, which not only enable DNA cleavage but also enable HDR with an exogenously added donor DNA template. Our mechanistic analysis of error-prone gene editing activity demonstrates how the unintended genetic outcomes are numerous, even when the gRNA and the target DNA do not align in perfect homologous register. Our system allows for visualization of the genetic diversity for all product molecules from these complex reactions, possibly reflecting the genetic effects of gene editing in a diverse human population. Whereas DNA cleavage alone can activate nonspecific repair systems, such as NHEJ, thereby creating resected or mutagenized DNA, our studies take it one step further to reveal how gRNA sequence variance does not inhibit precise or error-prone HDR.

The cell-free extract *in vitro* system enables a reductionist approach to the elucidation of the regulatory circuitry that controls the CRISPR-directed gene editing. As shown previously, NHEJ and MMEJ most likely promote indel formation and short fragment insertion, respectively.[17] Here, we emphasize that HDR and NHEJ take place in the same reaction mixture. Generally, we find that Cas12a catalyzes a higher degree of precise HDR, specifically when it is combined with a nonsense donor DNA strand. However, reactions with the Cas12a RNP and sense strand ODN exhibited reduced levels of HDR, whereas the majority of the population shows high levels of error-prone HDR products. This combination demonstrates an overall lower number of white colonies compared to other combinations of the genetic tools used in the present study. This curious observation may indicate that the S strand is serving to preserve the break site in such a way that it might enable the religation without resection or insertion. The low levels of white colonies generated in reactions driven by CRISPR/Cas9 complexes reflect the low levels of HDR gene editing activity. These outcomes hamper our ability to obtain statistically significant data, suggesting that the trend displayed by the Cas9/S strand combination is not an effective catalyst of precise HDR. Reactions in which Cas9 provides the nuclease activity do not support high levels of precise HDR, but most product molecules resulted in indels. This may be due to the structure of the termini created by the action of the nuclease, in the case of Cas9, a blunt end, which is less amenable to ssDNA annealing and strand invasion.[28]

We demonstrate that both CRISPR/Cas12a and CRISPR/Cas9 complexes are capable of cleaving target DNA, even when there are up to four mismatches present between the target and gRNA. As the number of mismatches increases from one to four, an increasing amount of nicked DNA and a decreasing level of fully linearized DNA are observed. Reactions containing Cas12a and the S strand are highly sensitive to the degree of mismatches in the gRNA, as one or two mismatches reduce the occurrence of precise HDR events dramatically; in these cases, the dominant product of the reaction is again indels, likely arising from the simultaneously active NHEJ process. The combination of Cas12a and the NS donor strand achieved high levels of HDR, even in the presence of several mismatches. CRISPR/Cas9, combined with the S strand, did exhibit HDR activity, even with 4 mismatched bases (see Table 2, C4). One could argue that in some cases, Cas9 could have remained bound to the cleaved ends of

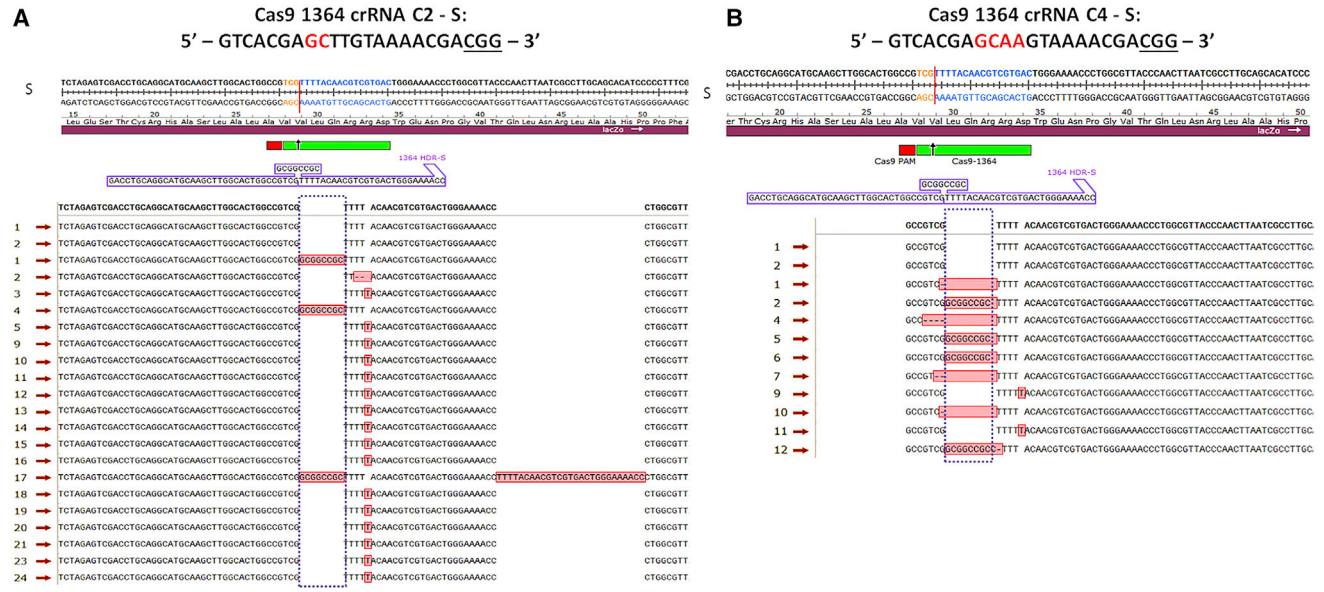

Cas9 1364HDR-S: C2 crRNA				
Colony	Total	HDR	Indel	WT
White	20	2	18	0
Blue	21	0	0	21

Cas9 1364 HDR-S: C4 crRNA				
Colony	Total	HDR	Indel	WT
White	10	3	7	0
Blue	22	0	0	22

Figure 4. CRISPR/Cas9 1364 Homology-Directed Repair Sense Strand Center Mutations C2, C4

The gRNA sequence is shown with mutated bases in red. The sense single-stranded oligonucleotide is shown to its complementary target site within the *lacZ* gene. (A) The C2 mutation showed that precise homology-directed repair occurred in two of the white colonies, whereas the remaining eighteen colonies present molecules with indels. (B) The C4 mutation showed precise homology-directed repair in three of the white colonies and the remaining seven white colonies harboring indels. The total number of blue and white colonies sequenced and which of those harbored precise homology-directed repair, indels, or wild-type molecules are shown.

the target duplex, thus accounting for the reduced activity levels shown. However, these experiments were repeated with multiple rounds of deproteinization, and the results remained the same. As described above, the total number of white colonies is low, and the results are not robust. Nonetheless, they support the notion that CRISPR/Cas-directed HDR can take place even when the gRNA is

Table 3. CRISPR/Cas12a and Cas9 Homology-Directed Repair Nonsense Strand Center Mutations

Cas12a 1364 HDR-NS: Center Mutations						Cas9 1364 HDR-NS: Center Mutations					
Mutation	Colony	Total	HDR	Indel	WT	Mutation	Colony	Total	HDR	Indel	WT
C0	White	20	16	4	0	C0	White	20	0	20	0
C0	Blue	26	0	0	26	C0	Blue	25	0	0	25
C1	White	19	14	5	0	C1	White	17	1	16	0
C1	Blue	21	0	0	21	C1	Blue	25	0	0	25
C2	White	20	14	6	0	C2[a]	White	17	3	14	0
C2	Blue	21	0	0	21	C2	Blue	25	0	0	25
C3[a]	White	18	11	6	1	C3	White	20	0	19	1
C3	Blue	26	0	0	26	C3	Blue	25	0	0	25
C4	White	2	1	0	1	C4	White	3	1	2	0
C4	Blue	21	0	0	21	C4	Blue	25	0	0	25
C5	White	0	0	0	0	C5	White	3	0	2	1
C5	Blue	20	0	0	20	C5	Blue	25	0	0	25

The total number of blue and white colonies is represented, along with the number of colonies found to have precise homology-directed repair, insertions or deletions (error-prone sequences), or wild-type molecules for Cas12a (left) and Cas9 (right) center mutations using the nonsense single-stranded oligonucleotide.

[a]Unique and precise homology-directed repair event.

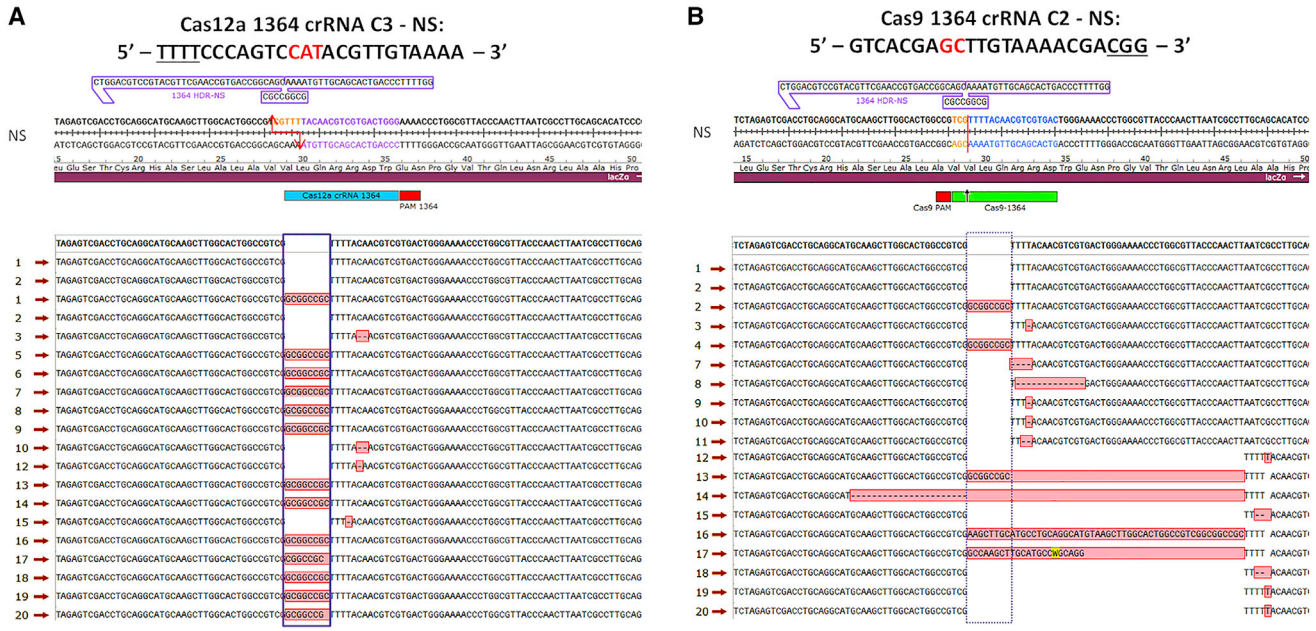

Cas12a 1364HDR-NS: C3 crRNA				
Colony	Total	HDR	Indel	WT
White	18	11	6	1
Blue	26	0	0	26

Cas9 1364 HDR-NS: C2 crRNA				
Colony	Total	HDR	Indel	WT
White	17	3	14	0
Blue	25	0	0	25

Figure 5. CRISPR/Cas12a C3 Mutation and Cas9 C2 Mutation Homology-Directed Repair Nonsense Strand

The gRNA sequence is shown with mutated bases in red. The tables below the center mutations demonstrate the total number of blue and white colonies sequenced and which of those sequences harbored precise homology-directed repair, indels, or wild-type molecules. (A) The Cas12a C3 mutation showed that precise homology-directed repair occurred in eleven of the white colonies sequenced, and the remaining show indel formation. (B) The Cas9 C2 mutation showed precise homology-directed repair occurring in three white colonies, whereas the remaining colonies show indel formation.

misaligned with the target site, a level of genetic infidelity that could elevate the propensity for inappropriate DNA insertion at unintended locations in the chromosome.

Our initial intent in developing the *in vitro* system was to examine details of the CRISPR/Cas gene editing reaction by taking a decidedly reductionist approach. We have found that the *in vitro* system accurately reflects reaction parameters described in cell-based systems, including (perhaps most importantly) a donor strand bias, in which the polarity of the donor strand enables higher levels of accurate gene editing.[25,29] We also found that NHEJ and HDR are active and competitive in the *in vitro* system, again reflecting the situation in cell-based models. Here in the present study, NHEJ and HDR (and perhaps MMEJ) pathways are active, and they likely compete for the target molecule. Furthermore, we demonstrated that double-strand breaks created by a programmable nuclease, CRISPR/Cas, are more effective in promoting successful gene editing as compared to single-agent approaches.[29] In this study, we demonstrate that Cas12a is more effective in promoting accurate HDR than its counterpart Cas9.[30] We are currently in the process of establishing a cell-based system that reflects the target sites and reaction conditions that we have established for the *in vitro* gene editing reactions. We will conduct an extensive side-by-side comparison for each of the phenomenon reported in previous work and in this paper to define specific connections between *in vitro* and cell-based assays. We recognize that developing correlations surrounding the topic of off-site mutagenesis between the *in vitro* system and the cell-based system will be limited, since the target size in the *in vitro* system is quite small.

Our results also reinforce the conclusions drawn by Boel et al.[6] in their elegant studies with CRISPR/Cas9-mediated HDR in zebrafish. These authors suggest that gene editing tools can produce complex mutational patterns, and the variability of these outcomes could occur by partial integration of repair template fragments.[6] Our mechanistic data confirm their observations, and we believe that single-stranded donor DNA may promote DNA synthesis-dependent strand annealing in such a way that unusual synthetic errors are introduced into the target DNA.[19] In our case, however, we see that these outcomes are heavily influenced by the polarity of the donor DNA strand. Whereas such strand bias has been reported extensively both *in vitro*[17] and *in vivo*,[30] the *in vitro* system does not fully recapitulate the obvious steric hindrance produced by the nucleosome and other chromatin-associated proteins. Thus, the influence of donor DNA strand bias could be amplified in the *in vitro* cell-free extract system. Whereas

Table 4. Statistical Analysis of CRISPR/Cas9 and CRISPR/Cas12a

Cas12a HDR-NS No Center Mutation Versus Cas9 HDR-NS No Center Mutation			
	HDR	Indel	Total
Cas12a HDR-NS	16	4	20
Cas9 HDR-NS	0	20	20
Total	16	24	40
			*p = 0.0001
Cas12a HDR-NS 1 Center Mutation Versus Cas9 HDR-NS 1 Center Mutation			
	HDR	Indel	Total
Cas12a HDR-NS 1 mutation	14	5	19
Cas9 HDR-NS 1 mutation	1	16	17
Total	15	21	36
			*p = 0
Cas12a HDR-NS No Center Mutation Versus Cas12a HDR-NS 1 Center Mutation			
	HDR	Indel	Total
Cas12a HDR-NS	16	4	20
Cas12a HDR-NS 1 mutation	14	5	19
Total	30	9	39
			p = 0.7164
Cas12a HDR-NS 2 Center Mutations Versus Cas9 HDR-NS 2 Center Mutations			
	HDR	Indel	Total
Cas12a HDR-NS 2 mutations	14	6	20
Cas9 HDR-NS 2 mutations	3	14	17
Total	17	20	37
			*p = 0.0026
Cas12a HDR-NS No Center Mutation Versus Cas12a HDR-NS 2 Center Mutations			
	HDR	Indel	Total
Cas12a HDR-NS	16	4	20
Cas12a HDR-NS 2 mutations	14	6	20
Total	30	10	40
			p = 0.7164
Cas12a HDR-NS 3 Center Mutations Versus Cas9 HDR-NS 3 Center Mutations			
	HDR	Indel	Total
Cas12a HDR-NS 3 mutations	11	6	17
Cas9 HDR-NS 3 mutations	0	19	19
Total	11	25	36
			*p = 0
Cas12a HDR-NS No Center Mutation Versus Cas12a HDR-NS 3 Center Mutations			
	HDR	Indel	Total
Cas12a HDR-NS	16	4	20
Cas12a HDR-NS 3 mutations	11	6	17
Total	27	10	37
			p = 0.4597

Fisher's exact test was used to determine if there was statistical significance between CRISPR/Cas12a and CRISPR/Cas9 homology-directed repair reactions, with and without mutations, using both the S and NS oligonucleotides. Each panel displays the category of each comparison, as well as the number of samples for homology-directed repair, indels, and the total number of samples analyzed. The *P*-values are set to $p < 0.01$, and statistically significant data are denoted by an asterisk.

HDR editing or error-prone HDR has been previously reported,[19,29,31,32] we extend those studies by providing some quantification to its randomness. More importantly, we find that gRNA heterology supports both precise and error-prone HDR when mismatched bases are present during initial complexation and alignment.

Based on previous information regarding the overall genetic variation of human genomes, it is likely that genetic variation can impact CRISPR/Cas activity as it relates to on- and off-target site specificity. Genetic variance at the on-target site, potentially inherent in the diversity of the targeted human population, could also greatly influence reaction efficiency. This could be significant at therapeutically implicated loci and loci with some sequence similarity.[11] Our data suggest that specific insertions in unwanted regions of the chromosome can take place even when a significant level of DNA heterology between the gRNA and the target exists. We are beginning to test these observations in a cell-based system that can recapitulate the sequence variability utilized in the *in vitro* studies. These functional outcomes of intended and collateral activities within the genome should raise caution regarding CRISPR-directed gene editing.

MATERIALS AND METHODS

Cell-free Extract Preparation

HEK cell-free extract was prepared following the technique outlined by Cole-Strauss et al.[33] The HEK cell line (American Type Cell Culture, Manassas, VA) was cultured, harvested at 4.5×10^6 cells, and washed with cold hypotonic buffer (20 mM of HEPES, 5 mM of KCl, 1.5 mM of $MgCl_2$, 1 mM of dithiothreitol [DTT], and 250 mM of sucrose). Cells were centrifuged based on their respective standard conditions, resuspended in cold hypotonic buffer without sucrose, and incubated on ice for 15 min before being lysed by 25 strokes of a Dounce homogenizer. Cytoplasmic fraction of enriched cell lysate was incubated on ice for 60 min and centrifuged for 15 min at 12,000 *g* at 4°C. The supernatant was then aliquoted and stored immediately at −80°C. The concentrations of the cell-free extract were determined using the Bradford assay.

In Vitro Reaction Conditions

The *in vitro* reactions used an RNP complex containing 10 pmol of purified AsCas12a (AsCpf1) with 10 pmol of a target-specific gRNA or an RNP complex with 10 pmol of *Streptococcus pyogenes* Cas9 (SpCas9) nuclease with 10 pmol of target-specific crRNA$^+$ tracrRNA (gRNA) (Integrated DNA Technologies, Coralville, IA). The cleavage reaction mixtures contained 500 ng (0.014 μM) of pHSG299 plasmid DNA (Takara Bio, Shiga, Japan) with 10 pmol of RNP mixed with a reaction buffer (100 mM of NaCl, 20 mM of Tris-HCl, 10 mM of $MgCl_2$, and 100 μg/mL of bovine serum albumin) and brought to a final volume of 20 μL. All cleavage reactions were incubated for 15 min at 37°C, and the DNA was recovered and purified using Zymo Research Select-A-Size DNA Clean & Concentrator (Zymo Research, Irvine, CA). The *in vitro* recircularization reaction contained DNA isolated and purified from the first cleavage reaction, 185 μg of cell-free extract supplemented with 400 cohesive end units of Quick T4 Ligase (New England Biolabs,

Ipswich, MA), a reaction buffer (20 mM of Tris, 15 mM of $MgCl_2$, 0.4 mM of DTT, and 1.0 mM of adenosine triphosphate), and single-stranded donor DNA templates (Integrated DNA Technologies, Coralville, IA) with homology arms on both sides of the target site; 100 pmol of oligonucleotide was added to the recircularization reaction. This secondary reaction was incubated at 37°C for 15 min, and then the DNA was isolated and purified using Zymo Research Select-A-Size DNA Clean & Concentrator (Zymo Research, Irvine, CA).

Transformation, Selection, DNA Isolation, and Analysis

Plasmid DNA recovered from the *in vitro* reactions was transformed into 50 μL of DH5α-competent *E. coli* (Thermo Fisher Scientific, Wilmington, DE) via heat shock transformation. Competent cells were incubated on ice for 30 min after the addition of purified DNA, heat shocked for 20 s at 42°C, placed on ice for 2 min, brought to a final volume of 1 mL in S.O.C. medium (Thermo Fisher Scientific, Wilmington, DE), and incubated for 1 h at 37°C, with shaking (225 rpm). 150 μL of undiluted competent cells was plated on media containing kanamycin antibiotics and incubated overnight at 37°C. The media are made using 500 mL agar, 500 μL of kanamycin antibiotics, and 2 mL of isopropyl β-D-1-thiogalactopyranoside (IPTG)/X-Gal solution (Thermo Fisher Scientific, Wilmington, DE). Single kanamycin-resistant colonies were selected based on their phenotypic color change (blue to white), and plasmid DNA was isolated using the ZymoPURE Plasmid Miniprep Kit (Zymo Research, Irvine, CA). The purified DNA was then analyzed via Sanger sequencing (GeneWiz, South Plainfield, NJ), and modifications were visualized using SnapGene software.

Statistical Analysis Using Fisher's Exact Test

The Fisher's exact test is a statistical analysis that establishes whether two category variables contain nonrandom associations when the total number of samples is low. This statistical test was used in Table 4 comparing several experimental combinations between Cas12a and Cas9.

SUPPLEMENTAL INFORMATION

Supplemental Information can be found online at https://doi.org/10.1016/j.omtn.2020.03.012.

AUTHOR CONTRIBUTIONS

E.B.K. and A.M.H. designed the experiments and wrote the manuscript. A.M.H. conducted the experiments. E.B.K., A.M.H., B.M.S., S.B., and G.T. have reviewed and approved the manuscript.

CONFLICTS OF INTEREST

S.B. and G.T. are employees of Novellus (Jerusalem, Israel). A.M.H., B.M.S., and E.B.K. have no conflict of interest or financial interest in associated companies.

ACKNOWLEDGMENTS

We thank our collaborators at Novellus and the entire Kmiec lab for their input and collaboration on the manuscript. We also show our appreciation to lab members Olivia Tharp, Kevin Bloh, and Kristen Pisarcik for their hard work and dedication to data analysis. This analysis was essential in answering pivotal questions and concerns pointed out by reviewers in the evaluation of the manuscript. This work was supported and funded by the Binational Industrial Research Development Foundation (BIRD Foundation) (1588).

REFERENCES

1. Barrangou, R., and Doudna, J.A. (2016). Applications of CRISPR technologies in research and beyond. Nat. Biotechnol. *34*, 933–941.
2. Prakash, V., Moore, M., and Yáñez-Muñoz, R.J. (2016). Current Progress in Therapeutic Gene Editing for Monogenic Diseases. Mol. Ther. *24*, 465–474.
3. Carroll, D. (2016). Genome editing: progress and challenges for medical applications. Genome Med. *8*, 120.
4. Doudna, J.A. (2015). Genomic engineering and the future of medicine. JAMA *313*, 791–792.
5. Jasin, M., and Haber, J.E. (2016). The democratization of gene editing: Insights from site-specific cleavage and double-strand break repair. DNA Repair (Amst.) *44*, 6–16.
6. Boel, A., De Saffel, H., Steyaert, W., Callewaert, B., De Paepe, A., Coucke, P.J., and Willaert, A. (2018). CRISPR/Cas9-mediated homology-directed repair by ssODNs in zebrafish induces complex mutational patterns resulting from genomic integration of repair-template fragments. Dis. Model. Mech. *11*, dmm035352.
7. Mali, P., Yang, L., Esvelt, K.M., Aach, J., Guell, M., DiCarlo, J.E., Norville, J.E., and Church, G.M. (2013). RNA-guided human genome engineering via Cas9. Science *339*, 823–826.
8. Hsu, P.D., Scott, D.A., Weinstein, J.A., Ran, F.A., Konermann, S., Agarwala, V., Li, Y., Fine, E.J., Wu, X., Shalem, O., et al. (2013). DNA targeting specificity of RNA-guided Cas9 nucleases. Nat. Biotechnol. *31*, 827–832.
9. Doench, J.G., Hartenian, E., Graham, D.B., Tothova, Z., Hegde, M., Smith, I., Sullender, M., Ebert, B.L., Xavier, R.J., and Root, D.E. (2014). Rational design of highly active sgRNAs for CRISPR-Cas9-mediated gene inactivation. Nat. Biotechnol. *32*, 1262–1267.
10. Sanjana, N.E., Shalem, O., and Zhang, F. (2014). Improved vectors and genome-wide libraries for CRISPR screening. Nat. Methods *11*, 783–784.
11. Lessard, S., Francioli, L., Alfoldi, J., Tardif, J.C., Ellinor, P.T., MacArthur, D.G., Lettre, G., Orkin, S.H., and Canver, M.C. (2017). Human genetic variation alters CRISPR-Cas9 on- and off-targeting specificity at therapeutically implicated loci. Proc. Natl. Acad. Sci. USA *114*, E11257–E11266.
12. Fu, W., O'Connor, T.D., Jun, G., Kang, H.M., Abecasis, G., Leal, S.M., Gabriel, S., Rieder, M.J., Altshuler, D., Shendure, J., et al.; NHLBI Exome Sequencing Project (2013). Analysis of 6,515 exomes reveals the recent origin of most human protein-coding variants. Nature *493*, 216–220.
13. Riaz, N., Wolden, S.L., Gelblum, D.Y., and Eric, J. (2016). Deregulation of STING signaling in colorectal carcinoma constrains DNA-Damage responses and correlates with tumorigenesis. HHS Public Access. *118*, 6072–6078.
14. Peplow, M. (2016). The 100,000 Genomes Project. BMJ *353*, i1757.
15. Doench, J.G., Fusi, N., Sullender, M., Hegde, M., Vaimberg, E.W., Donovan, K.F., Smith, I., Tothova, Z., Wilen, C., Orchard, R., et al. (2016). Optimized sgRNA design to maximize activity and minimize off-target effects of CRISPR-Cas9. Nat. Biotechnol. *34*, 184–191.
16. Sansbury, B.M., Wagner, A.M., Tarcic, G., Barth, S., Nitzan, E., Goldfus, R., Vidne, M., and Kmiec, E.B. (2019). CRISPR-Directed Gene Editing Catalyzes Precise Gene Segment Replacement *In Vitro* Enabling a Novel Method for Multiplex Site-Directed Mutagenesis. CRISPR J. *2*, 121–132.
17. Sansbury, B.M., Wagner, A.M., Nitzan, E., Tarcic, G., and Kmiec, E.B. (2018). CRISPR-Directed *In Vitro* Gene Editing of Plasmid DNA Catalyzed by Cpf1 (Cas12a) Nuclease and a Mammalian Cell-Free Extract. CRISPR J. *1*, 191–202.
18. Sansbury, B.M., Hewes, A.M., and Kmiec, E.B. (2019). Understanding the diversity of genetic outcomes from CRISPR-Cas generated homology-directed repair. Commun. Biol. *2*, 458.

19. Rivera-Torres, N., Banas, K., Bialk, P., Bloh, K.M., and Kmiec, E.B. (2017). Insertional Mutagenesis by CRISPR/Cas9 Ribonucleoprotein Gene Editing in Cells Targeted for Point Mutation Repair Directed by Short Single-Stranded DNA Oligonucleotides. PLoS ONE *12*, e0169350.

20. Richardson, C.D., Kazane, K.R., Feng, S.J., Zelin, E., Bray, N.L., Schäfer, A.J., Floor, S.N., and Corn, J.E. (2018). CRISPR-Cas9 genome editing in human cells occurs via the Fanconi anemia pathway. Nat. Genet. *50*, 1132–1139.

21. Brachman, E.E., and Kmiec, E.B. (2002). The 'biased' evolution of targeted gene repair. Curr. Opin. Mol. Ther. *4*, 171–176.

22. Engstrom, J.U., Suzuki, T., and Kmiec, E.B. (2009). Regulation of targeted gene repair by intrinsic cellular processes. BioEssays *31*, 159–168.

23. Engstrom, J.U., and Kmiec, E.B. (2008). DNA replication, cell cycle progression and the targeted gene repair reaction. Cell Cycle *7*, 1402–1414.

24. Lin, S., Staahl, B.T., Alla, R.K., and Doudna, J.A. (2014). Enhanced homology-directed human genome engineering by controlled timing of CRISPR/Cas9 delivery. eLife *3*, e04766.

25. Bialk, P., Rivera-Torres, N., Strouse, B., and Kmiec, E.B. (2015). Regulation of Gene Editing Activity Directed by Single-Stranded Oligonucleotides and CRISPR/Cas9 Systems. PLoS ONE *10*, e0129308.

26. O'Geen, H., Henry, I.M., Bhakta, M.S., Meckler, J.F., and Segal, D.J. (2015). A genome-wide analysis of Cas9 binding specificity using ChIP-seq and targeted sequence capture. Nucleic Acids Res. *43*, 3389–3404.

27. Jiang, F., and Doudna, J.A. (2017). CRISPR-Cas9 Structures and Mechanisms. Annu. Rev. Biophys. *46*, 505–529.

28. Liu, J., Majumdar, A., Liu, J., Thompson, L.H., and Seidman, M.M. (2010). Sequence conversion by single strand oligonucleotide donors via non-homologous end joining in mammalian cells. J. Biol. Chem. *285*, 23198–23207.

29. Paix, A., Folkmann, A., Goldman, D.H., Kulaga, H., Grzelak, M.J., Rasoloson, D., Paidemarry, S., Green, R., Reed, R.R., and Seydoux, G. (2017). Precision genome editing using synthesis-dependent repair of Cas9-induced DNA breaks. Proc. Natl. Acad. Sci. USA *114*, E10745–E10754.

30. Wang, Y., Liu, K.I., Sutrisnoh, N.B., Srinivasan, H., Zhang, J., Li, J., Zhang, F., Lalith, C.R.J., Xing, H., Shanmugam, R., et al. (2018). Systematic evaluation of CRISPR-Cas systems reveals design principles for genome editing in human cells. Genome Biol. *19*, 62.

31. Boel, A., Steyaert, W., De Rocker, N., Menten, B., Callewaert, B., De Paepe, A., Coucke, P., and Willaert, A. (2016). BATCH-GE: Batch analysis of Next-Generation Sequencing data for genome editing assessment. Sci. Rep. *6*, 30330.

32. Gratz, S.J., Cummings, A.M., Nguyen, J.N., Hamm, D.C., Donohue, L.K., Harrison, M.M., Wildonger, J., and O'Connor-Giles, K.M. (2013). Genome engineering of Drosophila with the CRISPR RNA-guided Cas9 nuclease. Genetics *194*, 1029–1035.

33. Cole-Strauss, A., Gamper, H., Holloman, W.K., Muñoz, M., Cheng, N., and Kmiec, E.B. (1999). Targeted gene repair directed by the chimeric RNA/DNA oligonucleotide in a mammalian cell-free extract. Nucleic Acids Res. *27*, 1323–1330.